complicated than one involving disproportionation: One possibility may involve the oxidation of water. In the presence of alcohol, the ratios of $\Delta[\mathrm{Pt(II)}]/[e_{\mathrm{aq}}^-]$ were near a value of 0.5/1. However, the kinetic evidence for the reactions of A_1 and A_2 with alcohol radical clearly indicates that the formation of Pt(II) resides not in disproportionation between Pt(III) species but rather in different processes.

Acknowledgment. We wish to thank the Natural Sciences and Engineering Research Council of Canada for financial support and the University of Saskatchewan for a scholarship (for H.M.K.). W.L.W. wishes to express his gratitude to the Hahn-Meitner-Institut and to the University of Saskatchewan for assistance and for the opportunity to spend periods of study at the former Institution.

Registry No. $\mathrm{Pt(NH_3)_4(H_2O)(OH)^{2+}}$, 80243-23-8; $\mathrm{Pt(NH_3)_4(OH)_2^+}$, 80243-24-9; $\mathrm{Pt(NH_3)_4(H_2O)_2^{3+}}$, 80243-25-0; $\mathrm{[Pt(NH_3)_4](ClO_4)_2}$, 21285-67-6; *trans*-$\mathrm{[Pt(NH_3)_4(OH)_2](ClO_4)_2}$, 80243-26-1.

Contribution from Chemistry Department A, Technical University of Denmark, DK-2800 Lyngby, Denmark, and from Chemical Department I, H. C. Ørsted Institute, University of Copenhagen, DK-2100 Copenhagen, Denmark

Lower Oxidation States of Sulfur. 2. Spectrophotometric, Potentiometric, and ESR Study of the Sulfur–Chlorine System in Molten NaCl–AlCl$_3$ (37:63 mol %) at 150 °C

RASMUS FEHRMANN,*[1a] NIELS J. BJERRUM,*[1a] and ERIK PEDERSEN[1b]

Received January 26, 1981

Three different cationic species have been produced either by anodic oxidation or by reaction between chlorine and elemental sulfur in a NaCl–AlCl$_3$ (37:63 mol %) melt at 150 °C. Two of the species found have been identified as the radicals S_4^+ and S_8^+. No ESR signals were found for the third species, and its oxidation state is most likely $+^1/_6$, indicating that the formula may be S_{12}^{2+}. The optical spectra of the three species were calculated from measured spectra.

Introduction

In a previously published paper[2] it was shown that by anodic oxidation of sulfur it was possible to form four different cationic species in an acidic NaCl–AlCl$_3$ (37:63 mol %) melt at 150 °C. The oxidation states for the four species were found to be +4, +2, and, most likely, +1 and $+^1/_2$ corresponding to the formation of S(IV), S(II), and, possibly, S_2^{2+} and S_4^{2+}. The present investigation concerns the less oxidized forms of sulfur produced in this melt. It will be shown that two cationic radicals, S_4^+ and S_8^+, exist in the melt besides elemental sulfur and a diamagnetic species, which most likely can be formulated as S_{12}^{2+}. The latter species is analogous to the selenium species Se_{12}^{2+}, which together with Se_4^{2+}, Se_8^{2+}, and Se_{16}^{2+} was identified (with good probability) in the NaCl–AlCl$_3$ (37:63 mol %) melt.[3,4] Sulfur species with formal oxidation states $+^1/_4$ and $+^1/_8$ have previously[5] been proposed to exist in NaCl–AlCl$_3$ (37:63 mol %). This investigation did not, however, include a quantitative treatment of the spectral data because of the rather great uncertainty in the spectra. The present spectrophotometric investigation was performed with a much better signal to noise ratio of the recorded spectra and is based on a greater number of spectra.

On the basis of electrochemical investigations[6] of elemental sulfur in the NaCl–AlCl$_3$ (37:63 mol %) melt, the existence of the species S_8^+ and S_8^{2+} has recently been proposed. It should, however, be noted that intermediate species produced on an electrode surface may not be those present at equilibrium. Attempts to isolate compounds containing low oxidation states of sulfur from the system (S_2Cl_2 + 2AlCl$_3$) + S_8 (with up to 87 mol % sulfur) by cooling the wine-red liquid mixture from 150 °C failed (only elemental sulfur was recovered).[7] This melt was neutral in the sense of chlorobasicity compared to the more acidic melt used in the present work. This fact might explain why no blue color was observed since low oxidation states usually are stable only in acidic media.

The nature of the brown, green, blue, and yellow solutions of sulfur in oleum has been the subject of much controversy since they were first reported in 1804.[8] Much later two paramagnetic species were proposed to exist in these solutions.[9] From ESR measurements it was found that one had a *g* value around 2.016 and the other a *g* value around 2.026.

Several authors have investigated these two radicals (called R_1 and R_2, respectively) by ESR spectroscopy on oleum solutions of sulfur and sulfur enriched with ^{33}S. There has been especially much discussion about the formula for R_1 (in oleum or fluorosulfuric acid), which has been proposed to be S_2^+,[10] S_4^+,[11-15] S_5^+,[16,17] S_7^+,[16] or S_8^+.[18] R_2 has been much less investigated, and only a few formulas for R_2 such as S_n^+,[14] (open chain radical) or S_8^+,[13] have been proposed. The diamagnetic species S_4^{2+}, S_8^{2+}, and S_{16}^{2+} (see footnote 31) have been isolated and characterized[12,19] in crystals with SO_3F^-, AsF_6^-, SbF_6^-, and $Sb_2F_{11}^-$ as anions. These sulfur species have also been proposed[13,20] to exist in oleum solutions, and the equilibria $S_8^{2+} \rightleftarrows 2S_4^+$ and $S_{16}^{2+} \rightleftarrows 2S_8^+$ have been suggested to account for the observed increase in paramagnetism with increasing temperature in oleum solutions[13,14] and in fluorosulfuric acid.[11] The contradictory conclusions of the different

---

(1) (a) Technical University of Denmark. (b) University of Copenhagen.

(2) Fehrmann, R.; Bjerrum, N. J.; Poulsen, F. W. *Inorg. Chem.* **1978**, *17*, 1195.

(3) Fehrmann, R.; Bjerrum, N. J.; Andreasen, H. A. *Inorg. Chem.* **1975**, *14*, 2259.

(4) Fehrmann, R.; Bjerrum, N. J. *Inorg. Chem.* **1977**, *16*, 2089.

(5) Bjerrum, N. J. "Characterization of Solutes in Non-Aqueous Solvents"; Mamantov, G., Ed.; Plenum Press: New York, 1978; pp 251–271.

(6) Marassi, R.; Mamantov, G.; Matsunaga, M.; Springer, S. E.; Wiaux, J. P. *J. Electrochem. Soc.* **1979**, *126*, 231.

(7) Corbett, J. D. *Prog. Inorg. Chem.* **1976**, *21*, 129.

(8) Bucholz, C. F. *Gehlen's Neues J. Chem.* **1804**, *3*, 7.

(9) Gardner, D. M.; Fraenkel, G. K. *J. Am. Chem. Soc.* **1956**, *78*, 6411.

(10) McNeil, D. A. C.; Murray, M.; Symons, M. C. R. *J. Chem. Soc.* **1967**, 1019.

(11) Gillespie, R. J.; Passmore, J. *J. Chem. Soc. D* **1969**, 1333.

(12) Gillespie, R. J.; Passmore, J.; Ummat, P. K.; Vaidya, O. C. *Inorg. Chem.* **1971**, *10*, 1327.

(13) Gillespie, R. J.; Ummat, P. K. *Inorg. Chem.* **1972**, *11*, 1674.

(14) Giggenbach, W. F. *J. Chem. Soc. D* **1970**, 852.

(15) Beaudet, R. A.; Stephens, P. J. *J. Chem. Soc. D* **1971**, 1083.

(16) Symons, M. C. R.; Wilkinson, J. G. *Nature (London)* **1972**, *236*, 126.

(17) Low, S. H.; Beaudet, R. A. *J. Am. Chem. Soc.* **1976**, *98*, 3849.

(18) Stillings, M.; Symons, M. C. R.; Wilkinson, J. G. *J. Chem. Soc. D* **1971**, 372; *J. Chem. Soc. A* **1971**, 3201.

(19) Davies, C. G.; Gillespie, R. J.; Park, J. J.; Passmore, J. *Inorg. Chem.* **1971**, *10*, 2781.

(20) Stephens, P. J. *J. Chem. Soc. D* **1969**, 1496.

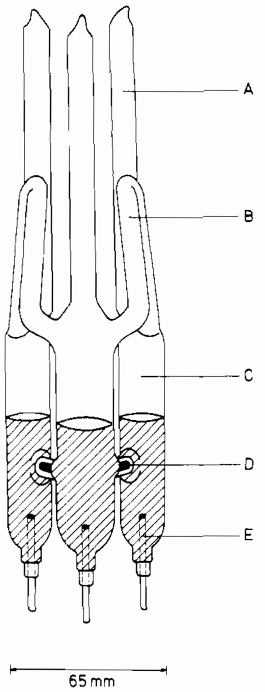

Figure 1. Three-chamber electrochemical cell: A, sealed loading tube; B, tube for pressure equalization; C, electrode chamber; D, porous plug; E, glassy carbon electrode.

authors might be due to the fact that equilibrium between the lower oxidation states in the oleum solutions is never obtained since the solute sulfur is slowly oxidized by the solvent, giving SO_2 as the final product.[13]

Experimental Section

Chemicals. Anhydrous $AlCl_3$ and NaCl were obtained as described previously.[2] The sulfur used was from Fluka (≥99.999%) and the enriched sulfur-33 (i.e., enriched to 48.56% ^{33}S) was from Oak Ridge National Laboratory, Oak Ridge, Tenn. The chlorine used was better than 99.9% (from Fluka). So that contamination of the anhydrous chemicals might be avoided, they were kept in sealed glass tubes until used. These were opened and handled only in a glovebox with a nitrogen atmosphere and with a water content of ca. 5 ppm. All weighings and additions to the cells used were performed in the same gloveboxes. The cells were thereafter sealed under vacuum or dry nitrogen.

Spectrophotometric Measurements. The two-chamber spectroelectrochemical cell used for these measurements was identical with the one previously described[2] but with an optical path length of 2 mm instead of 0.5 mm in order to obtain better accuracy for the bands of interest (with the same concentration range as previously used[2]).

The cell was placed in a spectrophotometer furnace[2] at 150 °C regulated to within ±0.1 °C. The dissolved elemental sulfur was oxidized anodically with a controlled-current controlled-time device (chronoamperostat) as earlier described.[21] After each change of composition by electrolysis the cell (and the spectrophotometer furnace) was rocked gently for 1–3 days until equilibrium was obtained (i.e., time-stable spectra). The furnace was then placed in a Cary 14R spectrophotometer; the spectra were recorded graphically and on paper tape by a Datex digital system connected to the spectrophotometer.

Potentiometric Measurements. The potentiometric measurements were performed in a three-chamber cell. The cell shown in Figure 1 was made of Pyrex and had a carbon rod (E) fused into the bottom of each cell compartment (C). The carbon rods (with diameter 3 mm, type V10 from le Carbone-Lorraine) were degassed in vacuum at 1200 °C for 12 h prior to use. The three chambers were connected through two ceramic porous plugs (D) with a pore size of 1.7–1.8 μm.

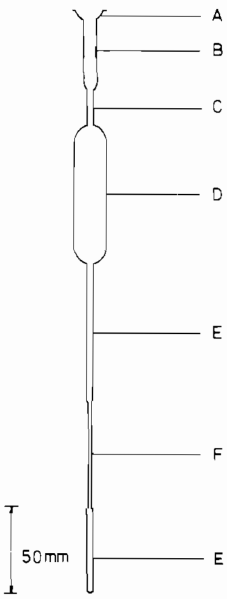

Figure 2. Cell used for ESR measurements: A, Rotulex joint of borosilicate glass; B, quartz–borosilicate-glass graded seal; C, place where cell is sealed off; D, mixing chamber; E, 5-mm quartz tubes; F, precision capillary tube.

The solid components were added to the three chambers through the loading tubes (A). The cell was evacuated, and the three tubes were sealed off under $^1/_2$ atm of dry nitrogen. The two small tubes (B) used for pressure equilibration were thereafter sealed off to prevent distillation of $AlCl_3$ (or volatile sulfur chlorides) from one chamber to the other. Addition of elemental sulfur was made to two of the chambers, leaving the third one still containing the pure melt only. The cell was thereafter placed in a furnace (described earlier[22]) the temperature of which was also regulated to within ±0.1 °C at 150 °C. The temperature of the furnace was measured to within ±0.5 °C by a calibrated chromel–alumel thermocouple. Contact between the carbon electrodes and chronoamperostat outside the furnace was made with silver wires connected to the carbon rods.

The electrolysis was performed between one of the two chambers containing sulfur (the anode chambers) and the chamber containing the pure melt (the cathode chamber). After each electrolysis the cell was rocked for 2–24 h until equilibrium was reached (indicated by measured potentials constant to within ±0.01 mV over a period of several hours).

ESR Measurements. The cell used for quantitative measurements is shown in Figure 2. The solid components that made up the melt were loaded through the joint (A) made of borosilicate glass. This greaseless type of joint (Rotulex ball joint) was necessary in order to add chlorine to the cell. The joint was connected to the quartz part of the cell through a quartz–borosilicate-glass graded seal (B). The tube (D) was used for equilibration of the melt prior to filling of the capillary (F), which was a 3.5-mm quartz tube with an inner diameter of 1.02 ± 0.01 mm from Wilmad Glass Co., Inc., Bueno, New Jersey.

Accurate addition of chlorine to obtain a given $S:Cl_2$ ratio was made in the following way. The appropriate amount of gaseous chlorine was transferred to a glass vessel (with a known volume), which was connected (through valves) to two separate gas cuvettes. The concentration was first determined with a homemade especially stabilized single-beam spectrophotometer where the absorbance was measured at 326 nm (the Cd line from an Osram Cd-10 lamp, selected by an interference filter). The amount of chlorine so determined was transferred to the evacuated cell by opening a valve located between the glass vessel and the cell and by cooling the lower part of the cell with liquid nitrogen. Finally a more accurate determination (i.e., ±1%) of the original chlorine concentration was made with the Cary 14R spectrophotometer.

The ESR spectra were recorded on a JEOL JES-ME-IX spectrometer operating in the X band. The cylindrical TE_{011} cavity was equipped with a gas-flow sleeve maintaining the capillary part of the sample tubes (Figure 2, F) at 150 ± 2 °C by the use of heated gas. The ESR cells were kept at 150 °C prior to transfer to the spectrometer. Conical Teflon inserts assured a reproducible position of the sample tubes inside the gas-flow sleeve. The internal diameter

---

(21) Andreasen, H. A.; Bjerrum, N. J. *Inorg. Chem.* **1975**, *14*, 1807.

(22) von Barner, J. H.; Bjerrum, N. J. *Inorg. Chem.* **1973**, *12*, 1891.

of the capillary was selected especially to optimize the sensitivity (i.e., selection of the best compromise between filling and Q factors of the cavity) since the dielectric losses were severe at the operating frequency. The top of the sample tube outside the cavity was heated separately to about 200 °C to prevent the melt from being blown out of the capillary due to differences in vapor pressures between top and bottom.

A single crystal of $CuCl_2 \cdot 2H_2O$ was placed in the cavity at room temperature and used as a sensitivity and field standard for each spectrum. By proper orientation its ESR spectrum consisted of a single line below 0.3 T. Solid DPPH and Mn^{2+} in MgO together with a cavity wavemeter served as means of calculating g factors.

The analog outputs from the spectrometer were digitized via a Tektronix 4051/4662 computer and transferred to a RC4000 computer for further data processing. The spectrum of each sample was recorded twice after intervals of some hours. Differences were minute after corrections. The spectra used in the curve-fitting procedure were average spectra (i.e., of the two recordings). Each spectrum typically consisted of 200 points.

General Considerations

The formality C' is defined as the initial molar amount of one of the added substances (in this work NaCl, $AlCl_3$, sulfur, and Cl_2) dissolved in 1 L of melt. The ratio between the formality of sulfur (always taken as S) and chlorine (taken as Cl_2) is denoted by the letter R. The amount of sulfur added was in the range 0.08–0.4% by weight, and the density of the melt was therefore assumed to differ only marginally from that of pure NaCl–$AlCl_3$ (37:63 mol %) melt at 150 °C. The density of the melt was obtained from the work of Boston.[23] The reaction $Al_2Cl_7^- + Cl^- \rightleftarrows 2AlCl_4^-$ ensured that the melt was well buffered with respect to the chloride activity. The variation in activity coefficients for solute species was neglected since the ionic strength of the solvent is high and the concentrations of solute species were low (less than 0.05 M).

Absorption Spectra. The formal absorptivity is defined as $A(lC')^{-1}$, where A is the measured absorbance corrected for the absorbance of cell and solvent and l is the optical path length. Before a quantitative treatment of the obtained spectra was made, a smoothing procedure was applied as described earlier.[3] In analogy to earlier work[2,3,24] a matrix equation based on the Bouguer–Beer law and the law of additive absorbances can be used:

$$[l_m C_{mi}][\epsilon_i(\nu_n')] = A_m(\nu_n') \qquad (1)$$

where l_m is the path length at the mth composition, C_{mi} is the concentration of the ith species for the mth composition, $\epsilon_i(\nu_n')$ is the molar absorptivity of the ith species at the wavenumber ν_n', and $A_m(\nu_n')$ is the total absorbance of the mth composition at the wavenumber ν_n'. The quantitative treatment is based on the $i - 2$ equilibria, which involve the i different species in the particular model chosen to explain the observed spectral changes. From arbitrarily chosen equilibrium constants (and from the formal concentrations of the materials that make up a melt) the concentration of each of the different species can be calculated for each composition. These concentrations together with the measured absorbances at the different wavenumbers and compositions are introduced into eq 1, and the "best" values (based on least-squares deviations) of $\epsilon_i(\nu_n')$ can be calculated as described earlier.[2,3,24] By systematic variation of the equilibrium constants the minimum deviation for the model involving the proposed species can be found. Earlier we were not generally able to examine models involving more than three species (i.e., one equilibrium), but in connection with the present work a new computer program has been developed, which can generally work with up to 8 species and 30 different compositions. The program incorporates Harwell standard routines[25] and contains new subroutines for calculations of concentrations based on a Newton-iteration procedure (for root estimation of an equation derived from the mass action expression after conversion to the equivalent logarithmic form).

As in previous works[2,3,24] an F test was used to distinguish between the various proposed models. The distinction is made between models with more or less probability than 90% (in comparison with the model with the lowest variance).

Cell Potentials. Previously[4,24] we have demonstrated that an electrochemical cell made of Pyrex with carbon electrodes fused into the bottom of the two chambers can be used to measure redox potentials of selenium and tellurium species. The cell used in the present work differs only by having a third chamber, which made it possible to electrolytically generate species independently in the two main chambers.

The composition of the part of the cell formed by these two chambers is

glassy carbon I	solution I: S_q^{r+} and S_v^{x+} in NaCl–$AlCl_3$ (37:63 mol %)	porous pin	solution II: S_q^{r+} and S_v^{x+} in NaCl–$AlCl_3$ (37:63 mol %)	glassy carbon II

where S_q^{r+} and S_v^{x+} are two important sulfur species, which under equilibrium conditions can be looked upon as a redox couple (r, q, v, and x are integers). I and II refer to the two main cell compartments. At each electrode we have the equilibrium

$$qS_v^{x+} \rightleftarrows vS_q^{r+} + ne^- \qquad (2)$$

where e is the electron and n is the number of electrons. By analogy with the selenium and tellurium systems,[4,24] the potential for such a cell is given by

$$\Delta E = \frac{RT}{F} \ln \frac{([S_q^{r+}]^{v/n})_{II}([S_v^{x+}]^{q/n})_I}{([S_q^{r+}]^{v/n})_I([S_v^{x+}]^{q/n})_{II}} \qquad (3)$$

where R, T, and F are the gas constant, the absolute temperature, and the Faraday constant, respectively.

ESR Spectra. The average ESR spectra were tentatively fitted by a least-squares method to a sum of two Lorentzian, two Gaussian, or a high-field Lorentzian and a low-field Gaussian line-shape functions, respectively. The function being minimized was

$$\sum_i (F(B)_{obsd} - F(B)_{calcd})^2/(\sigma^2(F) + (\partial F/\partial B)^2\sigma^2(B)) \qquad (4)$$

where $F(B)$ is the line-shape function (B is the magnetic field). Estimated values of the standard deviations $\sigma(B)$ and $\sigma(F)$ were typically 10^{-4} T and $10^{-2}F(B)$ (corresponding to a signal to noise level of 20 dB), respectively. The calculated values of relative variance per degree of freedom were around 1, 25, and 6 for the three types of line-shape functions, respectively. According to an F test this gives a significant evidence for a model including two Lorentzian functions as expected for rapidly tumbling radicals with no hyperfine couplings. Such a resolved spectrum is shown in Figure 8. An analysis of the distribution of signs of the differences between observed and calculated spectra showed that these were not randomly distributed. There was, however, no evidence for the presence of more than two lines in any of the spectra. In all attempts to fit the spectra to models with three lines, one of these was inevitably far out of the field range in question. It was obvious, however, that the high-field line ascribed to S_4^+ was almost perfectly described by a Lorentzian line shape, whereas the

---

(23) Boston, C. R. *J. Chem. Eng. Data* **1966**, *11*, 262.

(24) Fehrmann, R.; Bjerrum, N. J.; Andreasen, H. A. *Inorg. Chem.* **1976**, *15*, 2187.

(25) "Harwell Subroutine Library"; Scientific Administration Office, Atomic Energy Research Establishment: Harwell, Didcot, Berkshire, England; Nos. MA14AD, MA14BD, MC02BD, VG01AD, MC03AD, MB01BD.

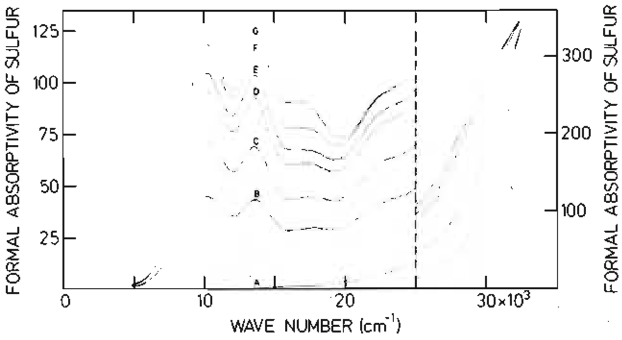

Figure 3. Series of spectra of different sulfur species in NaCl–AlCl$_3$ (37:63 mol %) at 150 °C produced by anodic oxidation of elemental sulfur. Note that two different absorptivity scales have been used. Formality of sulfur was 0.04009 (4). S:Cl$_2$ formality ratio: A, "∞"; B, 40.18; C, 24.19; D, 18.28; E, 16.12; F, 14.11; G, 12.10.

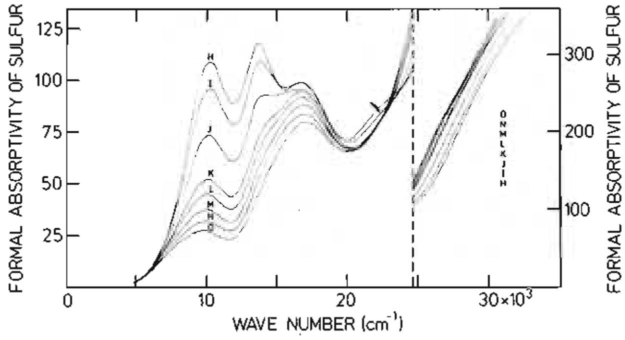

Figure 4. Series of spectra of different sulfur species in NaCl–AlCl$_3$ (37:63 mol %) at 150 °C produced by anodic oxidation of elemental sulfur. Note that two different absorptivity scales have been used. Formality of sulfur was 0.04009 (4). S:Cl$_2$ formality ratio: H, 11.09; I, 10.09; J, 9.07; K, 8.07; L, 7.56; M, 7.06; N, 6.56; O, 6.05.

low-field line ascribed to S_8^+ had a weak Gaussian character. The calculated *g* factors were 2.014 and 2.028, respectively.

The concentration of each species was calculated as being proportional to the double integral of each resolved Lorentzian line, since the spectra were recorded as first derivatives, and thus proportional to the product of the intensity peak to peak value and the square of the line widths. The standard deviations of these integrals were therefore almost solely determined by those of the half-widths.

Results and Discussion

Spectrophotometric Study of Sulfur Species Formed in the NaCl–AlCl$_3$ (37:63 mol %) Melt. A series of spectra obtained by anodic oxidation of sulfur in the NaCl–AlCl$_3$ (37:63 mol %) melt is shown in Figures 3 and 4. The formality of sulfur, C'_S, was 0.04009 (4) (i.e., 0.04009 ± 0.00004) and the temperature 150 °C. The oxidation was performed with a current of about only 2 mA for similar reasons as those previously described.[2] Even if chlorine is not produced in the melt initially, the sulfur species produced will be related to the calculated formality ratio R = S:Cl$_2$. The formality ratios corresponding to the obtained 28 spectra were in the range R = "∞" (i.e., the unoxidized sulfur solution) to R = 6.05 (1). For convenience only every second spectrum is shown in Figures 3 and 4. The spectra were corrected for the absorbance of cell and solvent.

In Figure 3 the spectrum of the pure sulfur solution marked A shows no band maxima and a low absorptivity up to ca. 25 × 10^3 cm^{-1}. After this wavenumber a considerable increase in absorptivity is observed. An example of the spectrum of slightly oxidized sulfur solution (i.e., R = 40.18) is spectrum B. In this spectrum two pronounced bands are found, one at 10.3 × 10^3 cm^{-1} (which is the most intense) and another at 13.6 × 10^3 cm^{-1}. Furthermore, two less intense bands are located around 17 × 10^3 and 22.7 × 10^3 cm^{-1}. Further oxidation down to an R value of 18.28 (spectrum D) results in a linear increase of the four bands. This can be verified for the band at 10.3 × 10^3 cm^{-1} by looking at Figure 5 where the formal absorptivity at this wavenumber in all measured spectra is plotted as a function of the formality ratio Cl$_2$:S. The formal absorptivity increases linearly up to R = ca. 18 (i.e., $1/R$ = Cl$_2$:S = 0.056), indicating[24] that only one species is obtained in this range (besides elemental sulfur). Similar plots at other wavenumbers show the same behavior. For convenience this first-found species will in the present article be labeled I.

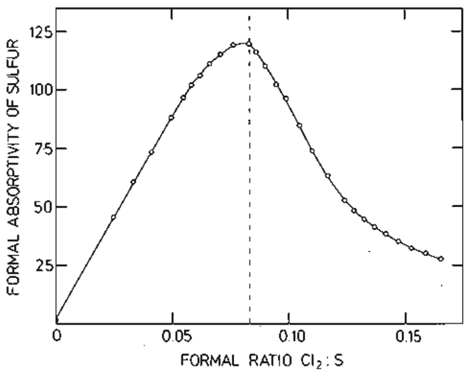

Figure 5. Relation between the formal absorptivity of sulfur measured at 10.3 × 10^3 cm^{-1} and the Cl$_2$:S formality ratio. Dashed line indicates formality ratio $^1/_{12}$.

Further oxidation from R = 18.28 (spectrum D) to R = 12.10 (spectrum G) results in a change in relative intensity between the band at 10.3 × 10^3 cm^{-1} and the band at 13.6 × 10^3 cm^{-1} (which actually shifts to ca. 13.8 × 10^3 cm^{-1}). Furthermore, in this R range a new band is formed, shifting to the band maximum at 17.4 × 10^3 cm^{-1} gradually to 16.7 × 10^3 cm^{-1}. In the same range the band at 22.7 × 10^3 cm^{-1} shifts to around 22.2 × 10^3 cm^{-1} and achieves its absolute maximum for R = 12.10 (spectrum G). It should also be noted that a weak shoulder appears around 29 × 10^3 cm^{-1} in spectrum E (R = 16.12) and that this shoulder is most pronounced for R = 12.10 (spectrum G) even if the total absorptivity (at 29 × 10^3 cm^{-1}) increases further in spectra G–O. From Figure 5 it is clear that the formal absorptivity of sulfur (at 10.3 × 10^3 cm^{-1}) deviates from its original linear dependence on the formality ratio Cl$_2$:S well before (i.e., around a Cl$_2$:S ratio of 0.056) it achieves its maximum value at Cl$_2$:S = ca. 0.0833 (or S:Cl$_2$ = 12) shown by the dashed line. Judged by the rather sharp break of the curve around Cl$_2$:S = 0.0833 (i.e., R = 12), the found deviation in the Cl$_2$:S range of ca. 0.056 to ca. 0.075 is due to the appearance of a new species (which for convenience in this paper will be labeled II). It is difficult from Figure 5 to locate where species I obtains its maximum concentration, but a likely value is for Cl$_2$:S = 0.0625 (i.e., R = 16). At Cl$_2$:S = 0.0833 (i.e., R = 12) species II then obtains its maximum concentration.

By further oxidation from R = 12.10 (spectrum G) to R = 6.05 (spectrum O) the band at 10.3 × 10^3 cm^{-1} is reduced under a gradual shift in band position to ca. 9.8 × 10^3 cm^{-1} combined with a reduction of the band at 13.8 × 10^3 cm^{-1}, which completely vanishes at R = 6.05 (spectrum O). Moreover, the other characteristic shoulders due to species II at 22.2 × 10^3 cm^{-1} and at ca. 29 × 10^3 cm^{-1} disappear. This is followed by the appearance of two other shoulders located around 26 × 10^{-3} and 31 × 10^{-3} cm^{-1}. Furthermore, these changes are accompanied by first an increase of the band at 16.7 × 10^3 cm^{-1} and then a decrease (and a shift to ca. 17.1 × 10^3 cm^{-1}).

Such behavior must be due to the formation of at least one new species (which for convenience we will label III) achieving

Table I. Spectrophotometric Measurements: Variances Obtained for Models[a] with Oxidation States in the Range $+^1/_6$ to $+^1/_{10}$[b]

oxidn state	formal charge 1+	2+	3+	4+
$+^1/_6$[c]	9.69×10^{-4}	9.93×10^{-4}	9.99×10^{-4}	9.99×10^{-4}
$+^4/_{25}$				3.19×10^{-4}
$+^3/_{19}$			3.23×10^{-4}	
$+^2/_{13}$		4.38×10^{-5}*		3.10×10^{-4}
$+^3/_{20}$			2.04×10^{-4}	
$+^4/_{27}$				2.20×10^{-4}
$+^1/_7$	2.85×10^{-5}*	2.71×10^{-5}*	6.44×10^{-5}	1.30×10^{-4}
$+^4/_{29}$				6.86×10^{-4}
$+^3/_{22}$			4.00×10^{-5}*	
$+^2/_{15}$		2.61×10^{-5}*		5.26×10^{-5}*
$+^3/_{23}$			3.18×10^{-5}*	
$+^4/_{31}$				3.34×10^{-5}*
$+^1/_8$	2.32×10^{-5}*	2.30×10^{-5}*	2.38×10^{-5}*	2.54×10^{-5}*
$+^4/_{33}$				3.28×10^{-5}*
$+^3/_{25}$			2.77×10^{-5}*	
$+^2/_{17}$		2.68×10^{-5}*		3.68×10^{-5}*
$+^3/_{26}$			4.33×10^{-5}*	
$+^4/_{35}$				5.22×10^{-5}*
$+^1/_9$	2.45×10^{-5}*	4.96×10^{-5}*	6.56×10^{-5}	6.56×10^{-5}
$+^4/_{37}$				8.36×10^{-5}
$+^3/_{28}$			8.60×10^{-5}	
$+^2/_{19}$		1.30×10^{-4}		1.01×10^{-4}
$+^3/_{29}$			1.11×10^{-4}	
$+^4/_{39}$				1.22×10^{-4}
$+^1/_{10}$	7.40×10^{-5}	1.29×10^{-4}	1.74×10^{-4}	1.49×10^{-4}

[a] Other species in the equilibria assumed to be S_8, S_{12}^{2+}, and S_4^+. [b] Number of spectra 14; number of different wavenumbers 79; wavenumber range 5.2×10^3 to 25.1×10^3 cm^{-1}; formality ratio (S:Cl$_2$) range "∞" to 11.09 (2); asterisks based on $F_{0.10}(10.10) = 2.32$, indicating models with higher probability than 90%. [c] Other species in the equilibrium are in this case assumed to be S_8 and S_4^+.

its maximum concentration in the above-mentioned range (i.e., $12.10 \leq R \leq 6.05$). It can be seen from Figure 5 that the curve seems to break off around a Cl$_2$:S ratio of 0.125 (i.e., $R = 8$), indicating that the maximum concentration of III is obtained at this formality ratio.

In the previously published article[2] a spectrum with $R = 6.17$ was shown. This spectrum is almost identical with the spectrum with $R = 6.05$ (spectrum O) in the present article. Previously the shoulders at 26.5×10^3 and 31.3×10^3 cm^{-1} were attributed to the proposed species S_4^{2+}. It therefore seems probable that the product of oxidation of species III is S_4^{2+}, which achieves maximum concentration at $R = 4$. This is, however, outside the investigated R range in the present paper.

From the above discussion it seems that there are at least three sulfur species (with oxidation states between zero and $+^1/_2$) present in the melt. The most likely oxidation state for species II is $+^1/_6$, whereas the oxidation states for species I and III cannot be obtained with the same accuracy as for species II. However, possible values are $+^1/_8$ and $+^1/_4$, respectively. So that a formulation might be given for the three species, the procedure based on the matrix equation described under the General Considerations was applied.

The procedure was the following. So that the numerical problems for the calculations might be avoided, the spectra are split up in two groups representing R ranges where not more than four species at a time are present in significant amounts. In the first range (R = "∞", spectrum A, to $R = 11.09$, spectrum H) a model with two three-species equilibria involving elemental sulfur, I, II, and III was proposed to explain the spectral changes. The model equilibria were of the type

$$hS_q^{r+} + jS_y^{z+} \rightleftarrows kS_v^{x+} \qquad (5)$$

where the lower-case letters are integers. In the calculations involving elemental sulfur this was given as S_8, since S_8 has been shown[26] to be the predominant form of sulfur found in NaCl–AlCl$_3$ (37:63 mol %) melts at 175 °C. The calculations were performed with spectrum A (Figure 3) as the spectrum for S_8. In this way by having an invariable spectrum for S_8 in the calculations, we could reduce the number of degrees of freedom. This is furthermore a reasonable procedure since spectrum A was obtained with a high degree of accuracy.

Table II. Spectrophotometric Measurements: Variances Obtained for Models[a] with Oxidation States in the Range $+^2/_{11}$ to $+^1/_8$[b]

oxidn state	formal charge 1+	2+	3+	4+
$+^2/_{11}$		2.88×10^{-4}		1.13×10^{-4}
$+^3/_{17}$			6.32×10^{-5}	
$+^4/_{23}$				7.28×10^{-5}
$+^1/_6$	2.56×10^{-5}*	2.32×10^{-5}*	2.50×10^{-5}*	2.41×10^{-5}*
$+^4/_{25}$				2.48×10^{-5}*
$+^3/_{19}$			2.52×10^{-5}*	
$+^2/_{13}$		2.80×10^{-5}*		2.52×10^{-5}*
$+^3/_{20}$			2.68×10^{-5}*	
$+^4/_{27}$				2.58×10^{-5}*
$+^1/_7$	3.32×10^{-5}*	2.99×10^{-5}*	2.98×10^{-5}*	2.59×10^{-5}*
$+^4/_{29}$				2.65×10^{-5}*
$+^3/_{22}$			3.43×10^{-5}*	
$+^2/_{15}$		4.83×10^{-5}*		2.84×10^{-5}*
$+^3/_{23}$			$4.05 \times 10^{\ 5}$*	
$+^4/_{31}$				3.12×10^{-5}*
$+^1/_8$[c]	1.03×10^{-4}	7.94×10^{-5}	7.82×10^{-5}	8.24×10^{-5}

[a] Other species in the equilibria assumed to be S_8, S_8^+, and S_4^+. [b] Number of spectra 14; number of different wavenumbers 79; wavenumber range 5.2×10^3 to 25.1×10^3 cm^{-1}; formality ratio (S:Cl$_2$) range "∞" to 11.09 (2); asterisks based on $F_{0.10}(10.10) = 2.32$, indicating models with higher probability than 90%. [c] Other species in the equilibrium are in this case assumed to be S_8 and S_4^+.

In Table I the variances are given for different models involving different formulas for species I with oxidation state in the range $+^1/_{10}$ to $+^1/_6$. As formulas for species II and III S_{12}^{2+} and S_4^+, respectively, are used. The formula for II is based on a comparison with the analogous selenium system where Se_{12}^{2+} was proposed to exist and the formula for species III is based on the result of the ESR measurements, which will be described later in this paper. From Table I it can be seen that several models fit the obtained spectra within 90% probability, but that models including only S_8, S_4^+, and a species with an oxidation state of $+^1/_6$ (e.g., S_{12}^{2+}) can be excluded since the variances are very high. This supports the existence of the proposed species with an oxidation state between zero and $+^1/_6$. The lowest variances are, furthermore, obtained for models with an oxidation state of $+^1/_8$. On the basis of a comparison with the analogous selenium system[3,4] and on the basis of the proposed existence[12] of the compounds $S_{16}(SbF_6)_2$ and $S_{16}(AsF_6)_2$ the best guess for species I is S_{16}^{2+} (see footnote 31). However, the ESR measurements described in this paper show the existence of a radical with a formal oxidation state of $+^1/_8$, which presumably is S_8^+. The two models involving either S_{16}^{2+} or S_8^+ have almost the same variances, so the spectrophotometric method cannot be used to distinguish between these models. Further, the spectra cannot exclude the existence of the equilibrium $S_{16}^{2+} \rightleftarrows 2S_8^+$, which has been proposed to exist in other media.[12] However, the potentiometric method later described clearly favors S_8^+ and excludes S_{16}^{2+}.

The procedure is now to examine different formulations for species II, while in the equilibria elemental sulfur is taken as S_8, species I as S_8^+, and species III as S_4^+. The result of these calculations is shown in Table II. As before, many models fall within the 90% probability range but the lowest variances are obtained for models with a formal oxidation state of $+^1/_6$. It should be noted that models including only S_4^+, S_8, and a

---

(26) Huglen, R.; Poulsen, F. W.; Mamantov, G.; Marassi, R. *Inorg. Nucl. Lett.* **1978**, *14*, 167.

Table III. Spectrophotometric Measurements: Variances Obtained for Models[a] with Oxidation States in the Range $+^1/_3$ to $+^1/_5$[b]

oxidn state	formal charge 1+	2+	3+	4+
$+^1/_3$	2.25×10^{-4}	8.90×10^{-3}	7.19×10^{-2}	2.05×10^{-1}
$+^4/_{13}$				9.41×10^{-2}
$+^3/_{10}$			2.48×10^{-2}	
$+^2/_7$		1.43×10^{-3}		6.90×10^{-2}
$+^3/_{11}$			3.31×10^{-3}	
$+^4/_{15}$				6.05×10^{-3}
$+^1/_4$	1.06×10^{-5}*	5.36×10^{-5}	3.79×10^{-4}	1.13×10^{-3}
$+^4/_{17}$				9.61×10^{-3}
$+^3/_{13}$			7.84×10^{-3}	
$+^2/_9$		8.01×10^{-3}		4.60×10^{-2}
$+^3/_{14}$			3.06×10^{-1}	
$+^4/_{19}$				1.89×10^{-1}
$+^1/_5$	8.80×10^{-3}	1.30×10^{-1}	6.73×10^{-1}	6.28×10^{-1}

[a] Other species in the equilibria assumed to be S_8^+, S_{12}^{2+}, and S_4^{2+}. [b] Number of spectra 13; number of different wavenumbers 79; wavenumber range 5.2×10^3 to 25.1×10^3 cm^{-1}; formality ratio (S:Cl$_2$) range 10.09 (2)–6.05 (1); asterisk based on $F_{0.10}$-(9.9) = 2.44, indicating models with higher probability than 90%.

species with oxidation state $+^1/_8$ do not fit the spectra well. This supports the qualitative interpretation of the spectra that claimed the existence of a species with the formal oxidation state of $+^1/_6$ (i.e., between $+^1/_8$ and $+^1/_4$). The minimum variance in Table II is obtained for S_{12}^{2+}, and this formula corresponds to Se_{12}^{2+}, which was proposed in the analogous selenium system on the basis of potentiometric[4] and spectrophotometric evidence.[3] In the selenium system (with the solvent NaCl–AlCl$_3$, 37:63 mol % at 150 °C) no ESR signal was found for a solution with $C'_{SeCl_4} = 0.003\,661$ reduced with elemental selenium to the formality ratio Se:SeCl$_4$ = 20.82. This solution contains a mixture of the three selenium species with formal oxidation states $+^1/_4$, $+^1/_6$, and $+^1/_8$, respectively, and the absence of ESR signals supports the previously[3,4] assigned formulas Se_8^{2+}, Se_{12}^{2+}, and Se_{16}^{2+} for the three species. Furthermore, the present ESR measurements on the S–Cl$_2$ system give no indication of a paramagnetic species with the formal oxidation state of $+^1/_6$. Therefore, the most likely formula for species II is S_{12}^{2+}.

Finally different formulas for species III were examined while the other species in the equilibria were taken as S_8^+, S_{12}^{2+}, and S_4^{2+}. The variance obtained for models with oxidation states in the range $+^1/_3$ to $+^1/_5$ are shown in Table III. The lowest variance is obtained for S_4^+, and furthermore no other model falls within the 90% probability range defined by the applied *F* test. This species has also been proposed[13] to exist in other media in equilibrium with the S_8^{2+} cation (i.e., $S_8^{2+} \rightleftarrows 2S_4^+$). A model including both S_8^{2+} and S_4^+ (besides S_8^+, S_{12}^{2+}, and S_4^{2+}) cannot be ruled out at the present time.

It should also be mentioned that the color of the melt during the stepwise oxidation in the present work (i.e., for "∞" $\leq R \leq 6.05$) changes from yellow to bluish green to blue and finally bluish yellow. The blue is also characteristic for sulfur dissolved in oleum and has been attributed[27] to the S_8^{2+} cation. However, on the basis of the present observations all of the three species (I, II, and III) seem to contribute to the blue color of solutions in chloroaluminate melts.

Potentiometric Study of Sulfur Species Formed in the NaCl–AlCl$_3$ (37:63 mol %) Melt. The measuring chamber and reference chamber in the three-chamber cell were loaded with elemental sulfur corresponding to a formality of sulfur of 0.090 91 (5) and 0.091 71 (5), respectively. The electrolytic oxidation of the sulfur solutions was performed with a current of about only 5 mA for the same reason as given earlier.[2] The solution in the reference chamber was oxidized only once and kept at the formality ratio S:Cl$_2$ of 40.26 (2) while this ratio for the solution in the measuring chamber was changed stepwise down to *R* = 0.502 (0). The third chamber contained as before the pure melt. After each oxidation the potential between measuring and reference electrodes was measured. In the present article the measurements in the range 36.24 (2) $\geq R \geq$ 20.13 (1) will be dealt with while the results of a quantitative treatment of the data for the whole *R* range will be given in a later article.[28] The measured potentials at the different *R* values are given in Table IV.

Table IV. Values of the Cell Potential at Different Formality Ratios S:Cl$_2$ in Molten NaCl–AlCl$_3$ (37:63 mol %) at 150 °C[a]

ΔE, mV	S:Cl$_2$	ΔE, mV	S:Cl$_2$	ΔE, mV	S:Cl$_2$
7.44	36.24 (2)	21.41	30.20 (2)	55.27	22.15 (1)
11.11	34.47 (2)	34.60	26.20 (1)	71.06	10.13 (1)
16.27	32.19 (2)				

[a] Measuring chamber $C'_S = 0.090\,91$ (5); reference chamber $C'_S = 0.091\,71$ (5) and formality ratio S:Cl$_2$ = 40.26 (2); third chamber pure melt.

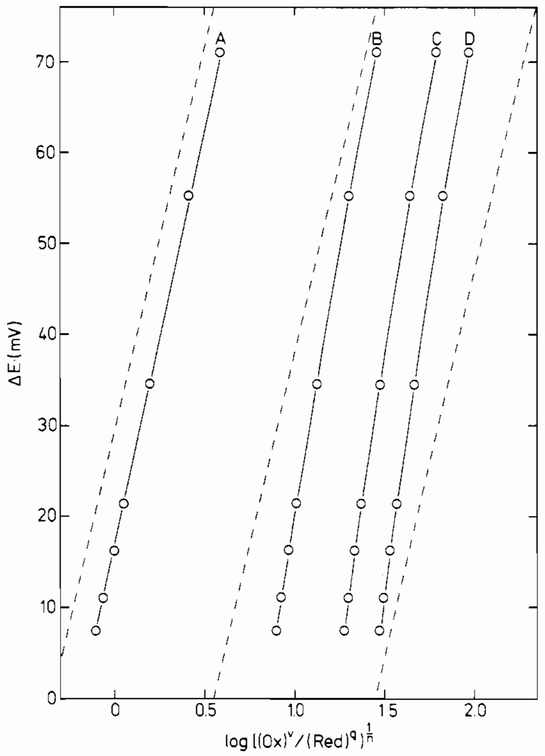

Figure 6. Relation between the measured ΔE taken from Table IV and the calculated value of log $((\mathrm{Ox})^v/(\mathrm{Red})^q)^{1/n}$. Formulas for Ox and Red and values of *v*, *q*, and *n*: (A) S_8^+, S_8, 1, 1, 1; (B) S_{16}^{2+}, S_8, 1, 2, 2; (C) S_{24}^{3+}, S_8, 1, 3, 3; (D) S_{32}^{4+}, S_8, 1, 4, 4. The dashed lines give the theoretical slope.

The cell potential is given by eq 3. If only two species (S_q^{r+} and S_v^{x+}) are present, the concentration of each species can be calculated from the formality of sulfur and the formality ratio S:Cl$_2$. In this case and if the model is correct a plot of the measured ΔE values vs. log $([S_q^{r+}]^v/[S_v^{x+}]^q)^{1/n}$ should give a straight line with the slope $RT(\ln 10)/F$. Such a plot is shown in Figure 6 for the data given in Table IV. In Figure 6, S_q^{r+} is designated Ox and S_v^{x+} Red, since S_q^{r+} has a higher oxidation state than S_v^{x+} in accordance with eq 2. The four plots in Figure 6 are based on four reaction schemes involving S_8 as Red and S_{8n}^{n+} (*n* = 1–4) as Ox. Since the concentrations of S_q^{r+} and S_v^{x+} in the reference chamber are constant, they are not included in the calculations. From the discussion of

---

(27) Malhotra, K. C.; Puri, J. K. *Indian J. Chem.* **1972**, *10*, 734.

(28) Fehrmann, R., manuscript in preparation.

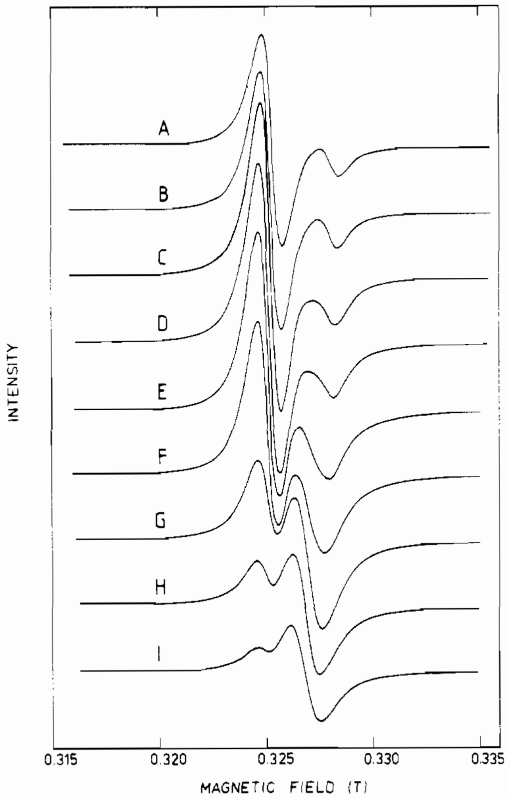

Figure 7. ESR spectra of the radical species produced in NaCl–AlCl$_3$ (37:63 mol %) at 150 °C by the reaction between sulfur and chlorine. Each spectrum is the average of two separate measurements. The formalities of sulfur were in the range 0.1816 (2)–0.1833 (2). S:Cl$_2$ formality ratios were as follows: A, 19.87; B, 18.05; C, 15.49; D, 13.39; E, 12.21; F, 10.04; G, 7.83; H, 5.79; I, 3.95.

the measured spectra it is clear that only elemental sulfur and one other species (species I) is present in the examined R range (i.e., $36.24 \leq R \leq 20.13$). It can be seen from Figure 6 that model A (with S_8^+ as the formula for species I) gives a straight line with a slope closer to the theoretical one (indicated by the dashed lines) than do the other models. This is of course strong evidence for S_8^+ being the formula of I. A reasonable explanation for the deviation between the estimated slope for model A and the theoretical slope is that not all of the elemental sulfur is present as S_8 but that small amounts are present as lower polymers. Suh a situation could not be ruled out in the Raman spectroscopic investigation[26] of elemental sulfur in the NaCl–AlCl$_3$ melt. On the basis of a least-squares deviation from a line with the theoretical slope the variances for models A–D were found to be 6.8×10^{-4}, 5.6×10^{-3}, 8.2×10^{-3}, and 9.8×10^{-3}, respectively. An F test showed that within 95% probability ($F_{0.05}(6.6) = 4.28$) any other model than S_8^+ could be excluded.

ESR Study of Sulfur Species Formed in the NaCl–AlCl$_3$ (37:63 mol %) Melt. In Figure 7 are shown nine different ESR spectra obtained by reaction of elemental sulfur with chlorine in NaCl–AlCl$_3$ (37:63 mol %) at 150 °C. The spectrum of a sample with an R value of 9.91 is omitted to avoid excessive data on one diagram. For the calculation of the molar amount of chlorine added (as described in the Experimental Section) the molar absorptivity of chlorine was determined by measuring the absorption of chlorine in a 1-cm cuvette at 21 °C and atmospheric pressure. The molar absorptivity at the band maximum of 328.8 nm was as an average of three measurements found to be 68.5 (1) L/(mol cm). This is somewhat higher (about 2%) than the value found previously.[29] However, any error of this magnitude will not be serious in the present work.

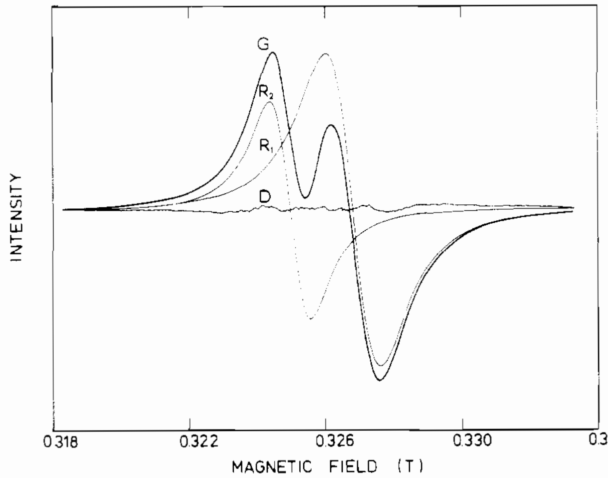

Figure 8. Resolution of the ESR spectrum (spectrum G) with S:Cl$_2$ = 7.83 into Lorentzian components, R$_1$ and R$_2$. Curve D (unsmoothed) shows the differences between observed and calculated spectra. A total of 184 points were included in the fitting procedure.

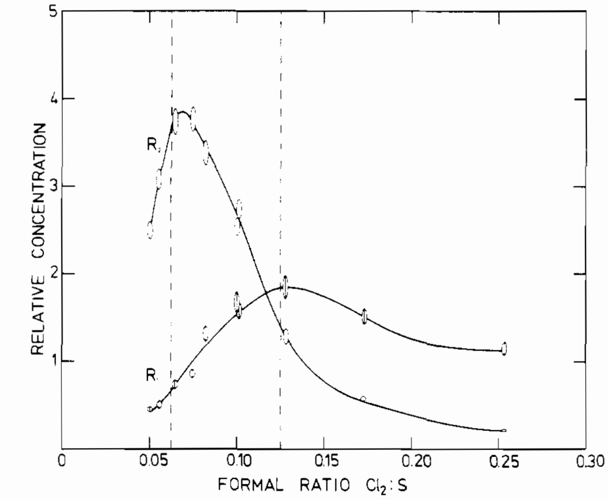

Figure 9. Relation between the calculated relative concentrations of the radical species R$_1$ and R$_2$ and the ratio Cl$_2$:S. The ellipsoids indicate the standard deviation. The dashed lines indicate the formality ratios $^1/_{16}$ and $^1/_8$, respectively.

The ESR spectra of the 10 samples having R values in the range 3.95–19.87 were corrected for intensity and field by comparison with that of the CuCl$_2$·2H$_2$O standard. An obvious interpretation is based on the assumption of two paramagnetic species (R$_1$ and R$_2$) in varying concentrations, both having $S = {}^1/_2$ corresponding to one unpaired electron but different g factors. The obtained spectra could not in any way be due to dissolved sulfur (e.g., S$_2$) since a solution being 0.02 M in elemental sulfur had no ESR signals. As discussed in the section on General Considerations the whole set of spectra could be fitted to a sum of two first-derivative Lorentzian line-shape functions with varying intensities (a resolved spectrum is shown in Figure 8). The g values were found to be 2.014 (1) and 2.028 (1) and the half-widths 1.53 (2) and 1.03 (1) mT, respectively. The corresponding concentrations calculated as the double integrals are shown in Figure 9 as functions of the Cl$_2$:S ratios.

It can be seen from Figure 9 that the maximum concentrations occur for one of the species at a Cl$_2$:S ratio close to 0.0625 corresponding to an oxidation state of $+{}^1/_8$ and for the other species at a Cl$_2$:S ratio close to 0.125 corresponding to an oxidation state of $+{}^1/_4$. Since there is no evidence for more

---

[29] Seery, D. J.; Britton, D. *J. Phys. Chem.* **1964**, *68*, 2263.

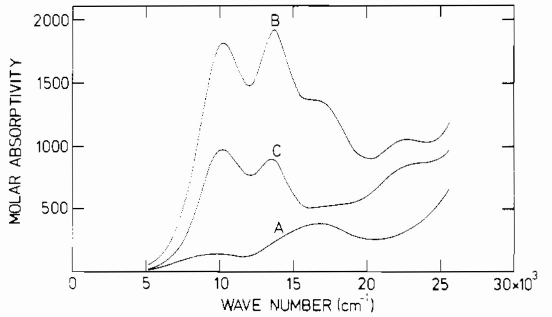

Figure 10. Calculated spectra of (A) S_4^+, (B) S_{12}^{2+}, and (C) S_8^+. Each spectrum was calculated on the basis of 28 measured spectra.

than one unpaired electron in each species, this shows that the species are most likely to be S_8^+ ($g = 2.028$ (1) and width 1.03 (1) mT) and S_4^+ ($g = 2.014$ (1) and width 1.53 (2) mT).

This result should be compared with those of ESR investigations on solutions of sulfur in oleum where species with very similar *g* factors have been described. In this system there is still a controversy concerning assignment of the oxidation states of the two species. However, on the basis of investigations of ^{33}S-enriched samples[16,17] S_5^+ rather than S_4^+ seems to be present in these melts.

In an attempt to determine the number of sulfur atoms in our two paramagnetic species we recorded ESR spectra of two samples containing 48.56% ^{33}S in the hope that they would show hyperfine coupling to this nucleus with $I = {}^3/_2$. The Cl_2:S ratios were chosen where the ESR spectra have maximum intensities (i.e., at 0.0625 and 0.1250). Unfortunately, the only consequence of isotopic substitution was a significant line broadening. We expected at least S_8^+ with a half-width of 1.03 mT to show partly resolved hyperfine lines in view of the hyperfine coupling constant around 0.9 mT found for the species in oleum solutions. Inequivalent couplings may account for the broad line features.

The large line widths found in our solvent may arise from solvation to $AlCl_4^-$ where Cl and Al have nuclear spins (${}^3/_2$ and ${}^5/_2$, respectively). Such interactions are very important for S_3^- in the same solvent. Here formation of $S_3AlCl_3^-$ (or $S_3AlCl_4^{2-}$) is likely as also indicated by the very large hyperfine coupling to the Al atom according to our recent investigations.[30] Such effects of solvation should be more pronounced for the smaller S_4^+ ion than for the S_8^+ ion, and this is actually observed since S_4^+ has the larger line width.

Conclusions

The combined results show that the species with the lowest valence next to elemental sulfur is S_8^+ and that the possible equilibrium $2S_8^+ \rightleftarrows S_{16}^{2+}$ is rather unimportant.[31] The species with oxidation state $+{}^1/_6$ is presumably S_{12}^{2+}, a diamagnetic species analogous to the earlier proposed selenium species Se_{12}^{2+}. The second radical is S_4^+. A possible existence of S_8^{2+} due to the equilibrium $2S_4^+ \rightleftarrows S_8^{2+}$ cannot be excluded, but the investigation shows that S_8^{2+} cannot be the dominant species with oxidation state $+{}^1/_4$.

Table V. *g* Values, Line Widths, and Absorption Maxima for Cationic Sulfur Radicals

	NaCl-AlCl$_3$ (37:63 mol %), 150 °C (this work)	15% oleum, room temp[13]	20% oleum, room temp[14]	65% oleum, room temp[17]
	"Sulfur Radical R$_1$"			
assignt	S_4^+	S_4^+	S_4^+	S_5^+
g	2.014 (1)	2.014	2.0131	2.0134 (3)
line width, T	15.3 (2) × 10^{-4}			
band max, 10^3 cm^{-1}	10.0 16.7		 17	
	"Sulfur Radical R$_2$"			
assignt	S_8^+	S_8^+	S_n^+	
g	2.028 (1)	2.027	2.0260	
line width, T	10.3 (1) × 10^{-4}			
band max, 10^3 cm^{-1}	10.3 13.5 18.0 23.3	10.6 13.9 23.8	10.6 13.9	

The calculated spectra of the three sulfur species S_8^+, S_{12}^{2+}, and S_4^+ are given in Figure 10. From this figure it can be seen that S_4^+ has band maxima at 10.0 × 10^3 and 16.7 × 10^3 cm^{-1}. The proposed species, S_{12}^{2+}, has band maxima at 10.3 × 10^3, 13.7 × 10^3 (the most intense) and 23.0 × 10^3 cm^{-1} and a shoulder at ca. 17.0 × 10^3 cm^{-1}, while the species S_8^+ has band maxima at 10.3 × 10^3 (the most intense) and 13.5 × 10^3 cm^{-1} and shoulders at ca. 18.0 × 10^3 (very weak) and ca. 23.3 × 10^3 cm^{-1}. It should be noted that the shape and band positions of the spectrum of S_{12}^{2+} can almost be created by a superimposition of the spectra of the two radicals. This might indicate that the structure of S_{12}^{2+} is a rather simple addition of the individual structures of the radicals. In Table V a comparison is made between the results of the present investigation and some investigations on oleum solutions containing sulfur species. From Table V it can be seen that the band positions and the *g* values assigned to S_4^+ and S_8^+ in this work are not far from the values assigned to R_1 and R_2 in oleum solutions. Furthermore, the general shape of the optical spectra obtained in the present work and the spectra given by Gillespie and Ummat[13] and Giggenbach[14] gives the impression that we are dealing with the same species in both solvents. However, the band maxima in the NaCl-AlCl$_3$ (37:63 mol %) melt seem to be shifted to somewhat lower wavenumbers compared with those in oleum solution. It should also be noted that the intensity of the ESR signals is markedly increased by increased temperature (from ca. −70 °C to room temperature) in oleum solutions, indicating that the concentrations of the radical species are increased at higher temperatures (e.g., also at 150 °C).

Acknowledgment. We wish to thank Statens teknisk-videnskabelige Forskningsråd for financial support.

Registry No. NaCl, 7647-14-5; AlCl$_3$, 7446-70-0; S_4^+, 12597-08-9; S_8^+, 11062-42-3; S_{12}^{2+}, 80263-39-4; S_8, 10544-50-0.

---

(30) Fehrmann, R.; von Winbush, S.; Papatheodorou, G.; Berg, R. W.; Bjerrum, N. J., to be submitted for publication in *Inorg. Chem.*

(31) After the present paper was submitted, we learned about an article by: Burns, R. C.; Gillespie, R. J.; Sawyer, J. F. *Inorg. Chem.* **1980**, *19*, 1423. Here it was pointed out that the compound previously thought to be $S_{16}(AsF_6)_2$ is in fact $S_{19}(AsF_6)_2$ (determined from three-dimensional X-ray diffraction data). Also features previously assigned to S_{16}^{2+} in oleum were attributed to the S_{19}^{2+} cation. S_{16}^{2+} thus appears to be an unimportant species in all the systems examined so far.